Journal of BUON **13:** 253-262, 2008
© 2008 *Zerbinis Medical Publications. Printed in Greece*

ORIGINAL ARTICLE

Dosimetry in translation total body irradiation technique: A computer treatment planning approach and an experimental study concerning lung sparing

Ch. Zabatis[1], Th. Koligliatis[2], St. Xenofos[2], K. Pistevou[3], K. Psarakos[4], A. Haritanti[5], K. Beroukas[1]

[1]1st Department of Radiation Oncology, "St. Savvas" Anticancer Hospital, Athens; [2]Department of Medical Physics, "St. Savvas" Anticancer Hospital, Athens; [3]Department of Radiotherapy, AHEPA Hospital, University of Thessaloniki, Thessaloniki; [4]Department of Medical Physics, AHEPA Hospital, University of Thessaloniki, Thessaloniki; [5]Department of Radiology, AHEPA Hospital, University of Thessaloniki, Thessaloniki, Greece

Summary

Purpose: *To describe and evaluate a method that uses a 3-dimensional (3D) treatment planning system (TPS) to determine the relative dose to the lung, and to study the beam filtration required for lung sparing in translation total body irradiation (TBI). Special dosimetric problems related to moving couch were also considered.*

Materials and methods: *The irradiation technique employed in our hospital is that of patient translation. The patient is positioned on a moving couch passing under a stationary Co-60 beam so that his/her entire body is irradiated. Measurements of basic data at source-skin distance (SSD)= 150 cm were used to implement the Co-60 TBI unit to TPS (THERAPLAN plus), which was then used in dose computations. Two stationary, opposed anterior-posterior (40× 40 cm) fields were employed to irradiate the Alderson phantom. The midline dose to either lung was computed and correction factors (CFs) were obtained that depend on the anatomy and densities of the tissues involved. These factors give the midline lung dose increase relative to the midline dose at the level of the mediastinum. Once the required lung dose was decided, the computed CF was used to estimate the filtration required from the measured broad beam attenuation data. The shielded lung dose distribution could be obtained from the TPS using a transmission corresponding to narrow beam geometry. To verify the TPS computations, measurements using a dosimeter and a diode system were carried out, employing solid water phantoms and the Alderson phantom.*

Results: *For the TPS employed, the computed midline CFs were lower than those measured in simple geometry phantoms for lung densities of 0.2-0.35 g/cm^3, by no more than 2%. For the Alderson phantom studied (lung density of 0.32 g/cm^3), the computed CF was 1.11, which was 2% higher than the measured value.*

Conclusion: *The advantages of a 3D TPS (dose distribution inside the lung, lung dose volume histograms [DVH], accurate attenuator shape from patient's anatomy etc.) allowed to study the lung dose in the Alderson phantom and to estimate the beam filtration required for lung sparing in TBI. The accuracy in lung dose computations, excluding the soft-tissue/lung interface was ≤ 5%, which is within the clinical dose requirements. This procedure has been applied to a number of patients prior to their irradiation. Computations and in vivo measurements were in good agreement.*

Key words: beam filtration, lung sparing, total body irradiation, treatment planning system

Introduction

In TBI the main critical organ is the lung, due to the risk for developing interstitial pneumonitis (50% mortality). Depending on the protocol followed, the lung may receive from 6 Gy in a single fraction to 12 Gy in as many as 6 fractions [1,2]. Lung dose tolerance depends on age, stage of disease, conditioning chemotherapy, fractionation scheme, dose rate etc. [3-7]. Fractionated schemes are now mostly applied and at-

Correspondence to: Thanos Koligliatis, PhD. Department of Medical Physics, "St. Savvas" Anticancer Hospital. 171, Alexandras Avenue, 115 22 Athens, Greece. E-mail: epappas@cc.uoa.gr

Received 07-08-2007; Accepted 13-11-2007

tention is given to lung sparing [8]. Our technique is a fractionated, low dose rate method of 12 Gy total dose in 5 days, 1 fraction/day.

TBI dosimetry presents special problems related to scattering conditions which become more important when large treatment distances and large field sizes are employed. These have been studied both theoretically and experimentally [7,9-20].

Various methods, involving *in vivo* measurements, have been applied to estimate the lung dose and the protection required or to verify their accuracy [10,13,18,21-26]. Thermoluminescence dosimetry (TLD), radiographic films, diodes and metal oxide semiconductor field effect transistor (MOSFET) dosimeters have been employed.

In this paper we describe a method that determines the shape and thickness of lead attenuator for lung sparing prior to patient irradiation. This is performed by studying the dose distribution in the thoracic region and the lung DVH with the aid of a 3D TPS. A Co-60 unit that contains the required data at an SSD=150 cm is implemented to our TPS. TPS computations that take place on a patient basis have many benefits including full patient dosimetric documentation. This is in accordance with the European Bone Marrow Transplantation (EBMT) protocol requirements. The patient's external contour and density inhomogeneities are known with accuracy, resulting in a desired dose distribution in each lung.

Materials and methods

Our irradiation technique is that of patient translation [14,27]. The translation technique may be considered as being equivalent to a stationary patient irradiated by a linearly "moving" beam. Percentage depth dose (PDD) data measured at a given SSD with a stationary and a "moving" field are not identical, the latter exhibiting increased PDD values compared to those from stationary fields (Figure 1). Due to beam divergence, points at greater depths remain in the beam for longer time. Simple geometry shows that at a depth "d" this increase is given by formula 1:

$$(SSD+d)/(SSD+d_{max})\sim 1+d/SSD \qquad (1)$$

However, when two opposed fields are used, the above effect results in dose distributions, along the central axis, which are practically the same (within 1%) for both types of beams, except for points near the body surface where the differences may reach 3% at d_{max}.

The gantry of the Co-60 radiotherapy unit (THERATRON-1000, Theratronics Int. Limited, Ontario, Canada) is adjusted so that the incident beam is normal to the patient who is positioned both supine and prone on a computer-speed-controlled couch at a source-to-couch distance of 170 cm. (Motorised patient translation couch, Jochen Barry GmbH, Essen, Germany). The couch speed is adjusted so that the required dose is delivered to a reference point, which is the midline at

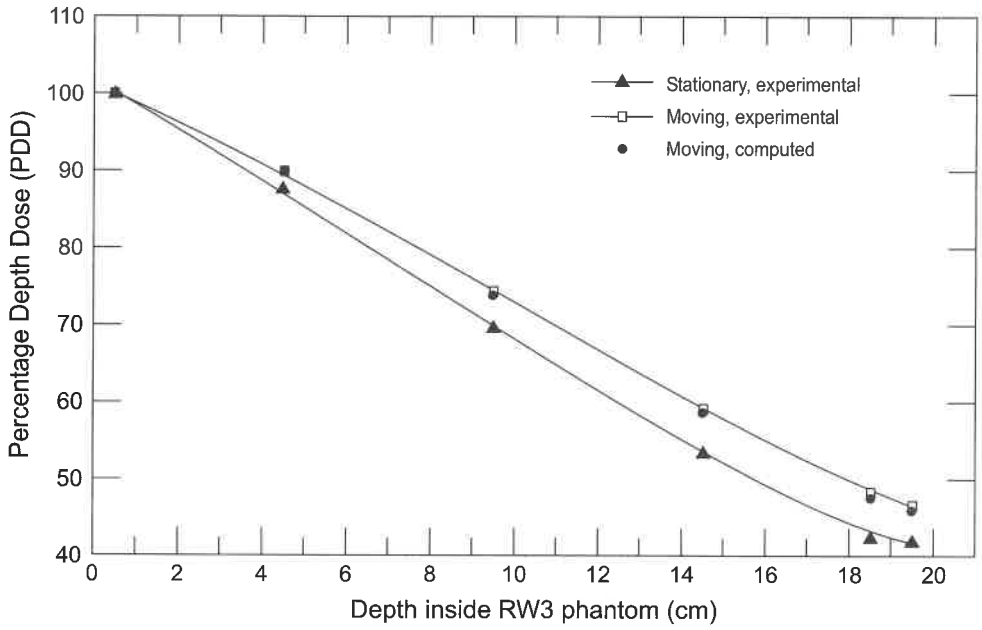


Figure 1. Comparison between PDD curves in: (a) stationary and (b) moving mode. The computed data have been obtained from the stationary beam once corrected by the geometric factor (see text). The curves are the fittings to experimental data (measurement errors are around 1%).

the level of the umbilicus. The speed of movement "u" is approximately given by the formula 2, where DR is the dose rate at the reference depth (d) for a stationary field of the same size and at the same SSD as the moving field, L_d is the field length at depth d and DF is the dose fraction required:

$$u = (DR \cdot L_d) / DF \qquad (2)$$

The field sizes employed are 40×40 cm at SSD= 150 cm in children and 50×40 cm in adults.

Implementation of the TBI unit to TPS

Earlier attempts, when normal treatment distance data (SSD=100 cm) were extrapolated and then used in TBI dose computations, led to serious errors due to poor scatter consideration (deviations up to 6%) [14,18,28,29]. These errors become greater when the lungs are involved (deviations up to 12%, in the middle of the lung, for AP/PA TBI) [16,18,19]. Therefore, radiation field data at an SSD value close to that in TBI and under similar scattering conditions should be used allowing lung dose distribution with acceptable accuracy. This is so because the central part of the profile of the stationary beam is very similar to that of the moving beam, whereas the profiles along the movement direction show a dose fall off in the moving beam occurring outside the fully scanned length. The same applies to other cross sections, provided they are located well within the field (within 65% of the field length the fall off of dose is about 2%) and the SSD is not very different from that at the central cross section, i.e. ±5 cm.

Field profiles, PDD curves and output factors were taken with a stationary beam at SSD=160 cm, using the water phantom system available (Therapy Beam Analyzer, PTW Freiburg, PTW, MP3) for a variety of field sizes (10×10, 20×20, 40×40, 50×50 and 60×60 cm). These data were implemented to TPS, THERAPLAN *plus*, version 2.1, Theratronics Int. Limited, Ontario, Canada. The photon beam inhomogeneity correction algorithm employed in 3D computations is the Equivalent Tissue Air Ratio method (ETAR) [30]. Data used for relative and absolute dose calculations have also been obtained from measurements using phantoms of solid water slabs irradiated on the couch, moving and stationary, under the TBI conditions.

TPS computations in the Alderson phantom

The TBI unit was first employed on a simulated treatment using the Alderson anthropomorphic phantom with a stated lung density of 0.32 g/cm^3. TPS computations were carried out using the CT images of the Alderson phantom, once the CT scanner had been calibrated with suitable electron density samples matching the electron densities met in clinical cases [31]. The purpose of these calculations was to obtain the relative increase of the dose to the lung, in relation to a reference point, which was then compared with that found experimentally.

The irradiation fields and the point of normalisation

In TPS, the irradiation fields (anterior and posterior) were arranged to cover the entire length of either lung as well as the width of the phantom. The computations were carried out for a field size of 40X40 cm at SSD=150 cm. The normalisation point was at the midline of the mediastinum, at the level of the central lung slice of the Alderson phantom (slice #17). This was done in order to avoid serious lung dose overestimate due to beam profile fall off.

In clinical practice the reference dose is specified at the midline at the level of the umbilicus (not at the mediastinum). If the midline dose values at these two points differ, the lung dose must be re-normalised relative to that of the umbilicus by multiplying the lung midline dose by D_{med}/D_{umb}, where D_{med} is the midline dose at the level of the mediastinum and D_{umb} is the midline dose at the level of the umbilicus.

From the dose distribution that refers to the stated slice, a CF, which is the ratio of the midline dose to lung to that of the reference point, is obtained. An average correction factor, CF_{av}, over the whole lung is also calculated.

Beam attenuation for lung protection - Attenuator optimisation

Lead or Cerrobend attenuators were used, placed on a thin Perspex plate fixed on the moving couch. The shape of the attenuator was decided with the aid of the Beam's Eye View (BEV) facility by the anatomy of each lung, which is clearly shown in the CT scans (Figure 2). Once the required average lung dose was stated, the necessary attenuator transmission was estimated from the average dose to each lung as a whole. The criterion to decide on the optimum attenuator shape and thickness was the optimum 3D dose distribution and the DVH of either lung, once clinical restrictions (minimum and maximum lung doses) had been considered. The attenuator shape was then back-projected to the skin and used on the simulator.

If the required lung dose was L (%) of the reference dose D_{ref} and CF was the increase in the midline lung dose relative to the reference point, calculated from the TPS, then the proper attenuator thickness

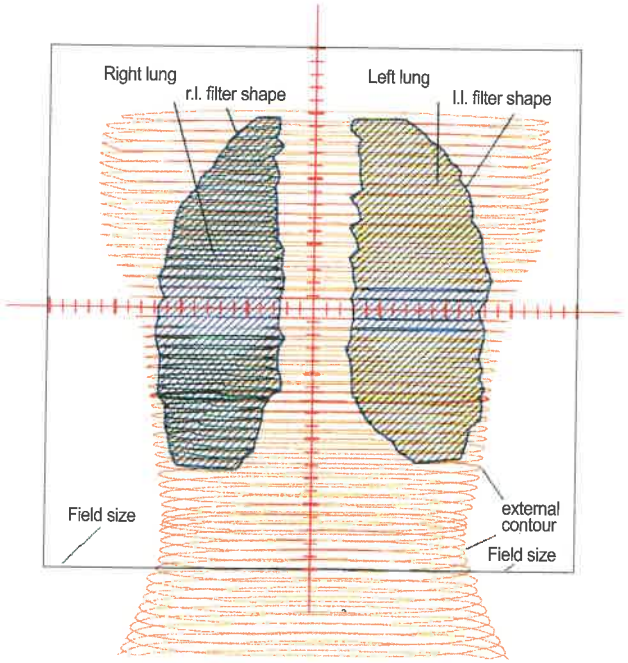


Figure 2. The shapes of the filters given with the aid of the BEV facility of the TPS. The filters are supposed to be placed on the skin of the patient. They can be drawn either automatically or manually, in collaboration with a radiotherapist. In this example each filter fully covers each lung.

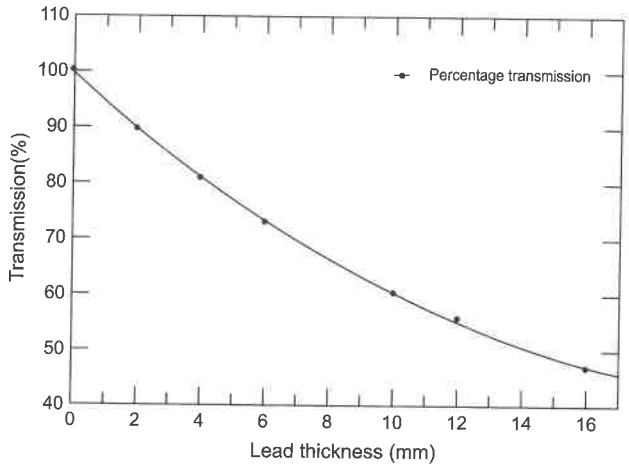


Figure 3. Percentage transmission against lead thickness variation under TBI conditions for a 40×40 cm field size (measurement errors ≤ 2%).

would result in a broad beam transmission (T) of T= L/CF (%) and might be obtained for a 40×40 cm field size from Figure 3. However, the TPS computations assume narrow beam transmission values and add the contribution due to scatter. The value of T to be employed in TPS computations should therefore be equal to the narrow beam transmission value, T_n. The value of T_n is based on lead attenuation coefficient of 0.656 cm^{-1}, which is the mean value of a number of narrow beam attenuation coefficients for Cobalt-60 radiation [32].

For the Alderson phantom study it was assumed that L=67% and the calculated CF was 1.11, resulting in T=60%. The required lead thickness was 10 mm (Figure 3) and T_n=52%. This T_n value should have resulted in a TPS calculated lung dose value under the attenuator very close to L=67%.

The lead thickness required

Transmission factors (T) were experimentally determined by dosimetric measurements at the midline of a 20 cm solid water phantom. Lead attenuators of various thickness, simulating the size of the lung (10×15 cm), were placed on the surface of the phantom which was irradiated on the moving couch by a 40×40 cm field at SSD=150 cm and the results are shown in Figure 3.

The lead linear attenuation coefficient for Co-60 under TBI conditions and a 40×40 cm field size, derived from the above data, was 0.51 cm^{-1}. This was 12% less than the value obtained by Van Dyk for the same field size (0.58 cm^{-1}) [18,32]. The corresponding difference in transmission for a 10 mm-lead attenuator was 7%. This was attributed to differences in the measurement geometry; the attenuator-to-detector distance was shorter (10 cm) and the field was only partially covered by the attenuator.

TPS computations and phantom measurements

The performance of the TPS itself was first tested through simulations of some experiments that had been carried out by Quast [33]. The phantoms simulated in the TPS were composed of solid water and a lung substitute that was centrally located relative to the incident beam (Figure 4), with densities of 0.1 g/cm^3 and 0.35 g/cm^3. The CFs obtained by Quast referred to the midline of the lung substitute, with and without the presence of lung (CF_o).

Patient irradiation was also simulated in the TPS using the Alderson phantom. This phantom was "irradiated" both in AP and PA directions at SSD=150 cm with a field size of 40×40 cm, first without lung protection and then with a 10 mm thick lead attenuator (corresponding to T_n= 52%) of suitable shape placed over the lungs. The TPS was first employed to obtain the thoracic region dose distribution, using T_n= 52% and then was compared with phantom measurements. Phantom dose measurements were carried out at the level of slice #17, using the silicon diode detector system available, calibrated under TBI conditions

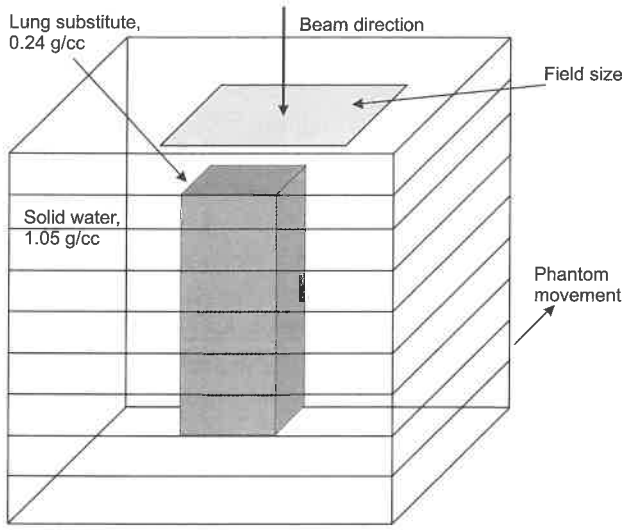


Figure 4. The experimental arrangement for measuring the effect of lung substitute on dose. The ratio of the dose in lung substitute to that in solid water, at the same geometrical point, is the lung correction factor CF_o.

against a SN4 dosimeter with the "Rigid" type 0.3 cm^3 cylindrical ionisation chamber (r=3 mm, wall material 0.35 mm PMMA [solid water] + 0.15 mm cap and wall thickness in surface density 54 mg/cm^2, Nr 23332 PTW, Freiburg, Germany). The calibration enabled the entrance dose, the exit dose, and the midline dose to be derived from diode measurements taken at the surface of the phantom and under the phantom inside special inserts. The same procedure was applied when lung substitutes had been employed (inhomogeneous phantom). Further corrections were necessary when the diodes were under the lead attenuators. No build-up cap was used and no chamber wall or stopping power values corrections were applied since the error in the relative lung dose measurements, under electronic equilibrium conditions, is around 1% [34]. The ratio of the dosimeter readings inside the lung substitute and at the centre of the solid water phantom at the same geometrical depth (phantom midline, Figure 4), was used as an estimate of the dose increase in the lung CF with no further corrections.

Results

Published measured CF_o [33] and our TPS computed CF_o are shown in Figure 5. For phantom thickness variation between 15 and 20 cm, lung thickness 5 cm less than that of the phantom and lung densities between 0.2 and 0.35 g/cm^3, the computed CF_o was smaller than the measured CF_o by < 2%. Using the data presented in Figure 5 for a phantom thickness of 20 cm and a lung thickness of 15 cm (a geometry that is quite

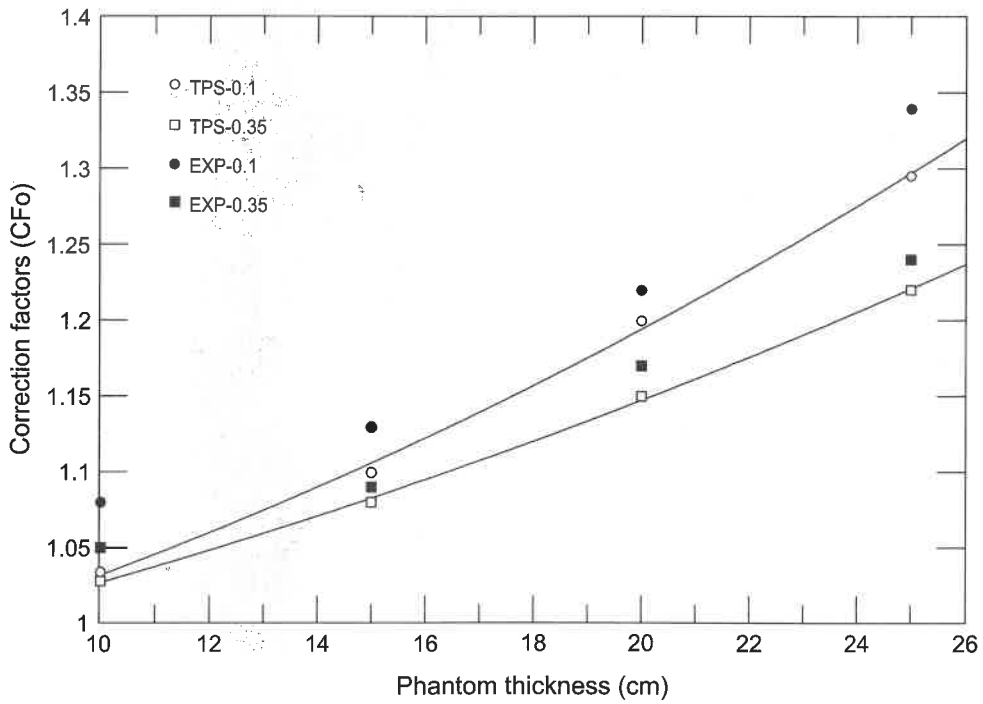


Figure 5. Comparison of our TPS computed CF_o (solid curves) and published measured CF_o for an inhomogeneous phantom consisting of solid water and lung substitute materials irradiated both in AP and PA directions under TBI conditions. Field size of 40×40 cm at SSD=160 cm. TPS refers to computed values and EXP to experimental data. The indices 0.1 and 0.35 denote the densities of the lung substitute in g/cm^3. The solid curves are the fittings to TPS computed values.

similar to that of slice #17 of the Alderson phantom, lung density=0.32 g/cm^3), an experimental correction factor CF_o=1.17 was obtained. This compares well with a CF_o=1.14 obtained for the same slice from TPS computations.

The measured CF values in the inhomogeneous solid water phantom (lung density of 0.24 g/cm^3, Figure 4) were 1.18 for phantom thickness of 20 cm and "lung" thickness of 15 cm, and 1.08 for corresponding thickness values of 15 cm and 9 cm, respectively. The corresponding values obtained using the TPS were 1.15 and 1.065. Therefore, the computed values were smaller than the measured values by about 2.5% and 1.5%, respectively.

Using the diode system, the measured increase in midline lung dose in slice #17 of the Alderson phantom, corresponding to the largest AP lung thickness relative to the midline dose at the mediastinum of the same slice, was 1.09 (range 1.08-1.10 in various experiments). The corresponding TPS computed CF for the midline dose of the lung (slice #17) was CF=1.11 (lung CF_{av}=1.10; Figure 6). Therefore, the computed value was greater than the measured one by about 2%, which was within the experimental error. The same difference was found in the case of the shielded lung.

The resulting dose distribution obtained for the Alderson phantom study (CF=1.11, L=67%, T=67/111 = 60%, T_n=52%) using a lung attenuator of 10 mm of lead, is shown in Figure 7. The corresponding computed DVH is shown in Figure 8. The DVH shows that 50% of the lung volume received a dose from 67% to just over 70% and the remaining 50% of the lung volume received a dose from 60 to 67%.

The 3D lung dose distribution of the 67% isodose surface shown in Figure 9 allows identifying regions of high and low dose. If the information obtained from DVH and 3D lung dose distribution does not comply with minimum and maximum lung doses, the shape and/or the thickness of the attenuator should be suitably modified.

The "moving beam" approach computations

In the translation TBI technique, the patient moves under a stationary beam. In TPS computations this is equivalent to a stationary patient under a moving beam. Simulation of the translation TBI technique in a TPS would offer certain advantages over the present method. This method could improve the calculation accuracy and enable the calculation of dose distribution over the entire body length (no beam profile fall-off along the direction of movement). The "moving beam" approach does not need lung dose re-normalisation. Also, study of the penumbra effect near the edges of each filter in the craniocaudal direction can only be performed through this method. This approach, which

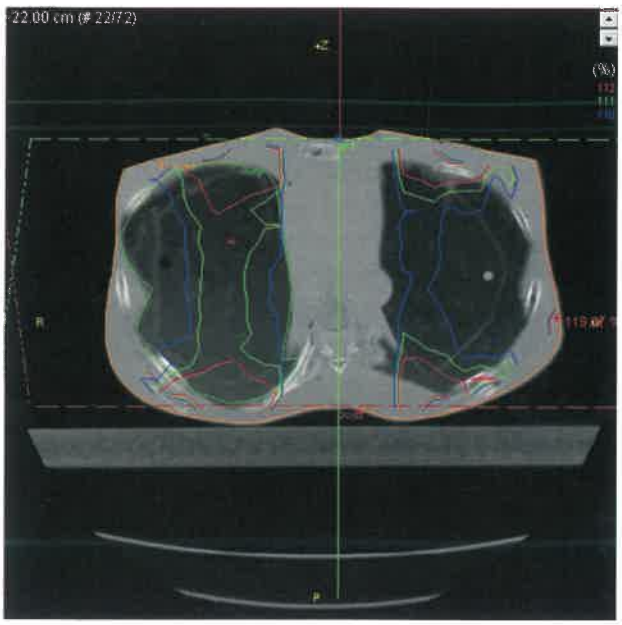


Figure 6. TPS calculated dose distribution inside a cross-section of the right lung (slice #17 of Alderson phantom) under TBI conditions. No lung attenuator is used. The midline right lung dose is very close to 111%. The isodoses are normalised to the midline of the mediastinum of the same slice.

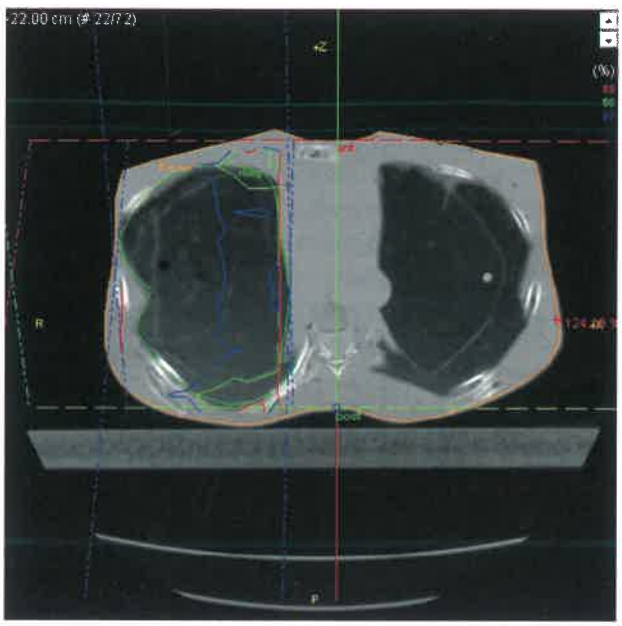


Figure 7. TPS calculated dose distribution inside a cross-section of the right lung (slice #17 of Alderson phantom) under TBI conditions. A 10 mm lead lung attenuator is used (Tn=52%) so that the midline lung dose is reduced to L= 67% of the mediastinum midline dose. Isodose curves of 67, 68 and 69% are shown.

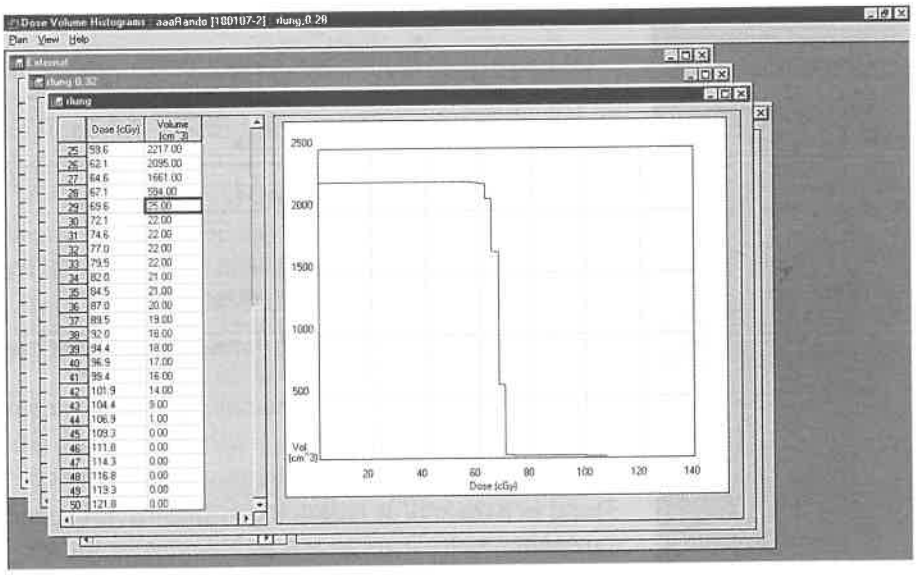


Figure 8. DVH of the right lung of the Alderson phantom obtained with the use of a 10 mm lead lung attenuator (T_n= 52%). The aim for a lung dose of 67% is reasonably achieved.

is called the "moving beam" approach, is briefly described below.

Twenty or more pairs of anterior and posterior beams were used in each case at a 2 cm-space interval along the part of the length of the patient's body that involved the lungs and the umbilicus (Figure 10). Each field size was adequate to cover the patient's width (40-60 cm) and the field length was set to 30 cm. The contribution of each beam (beam's intensity) was adjusted to account for differences in SSD compared to the SSD value at the level of the umbilicus.

The "moving beam" approach was in fact employed in 75 out of 85 patients irradiated so far (since September 2000) at the expense of time required for

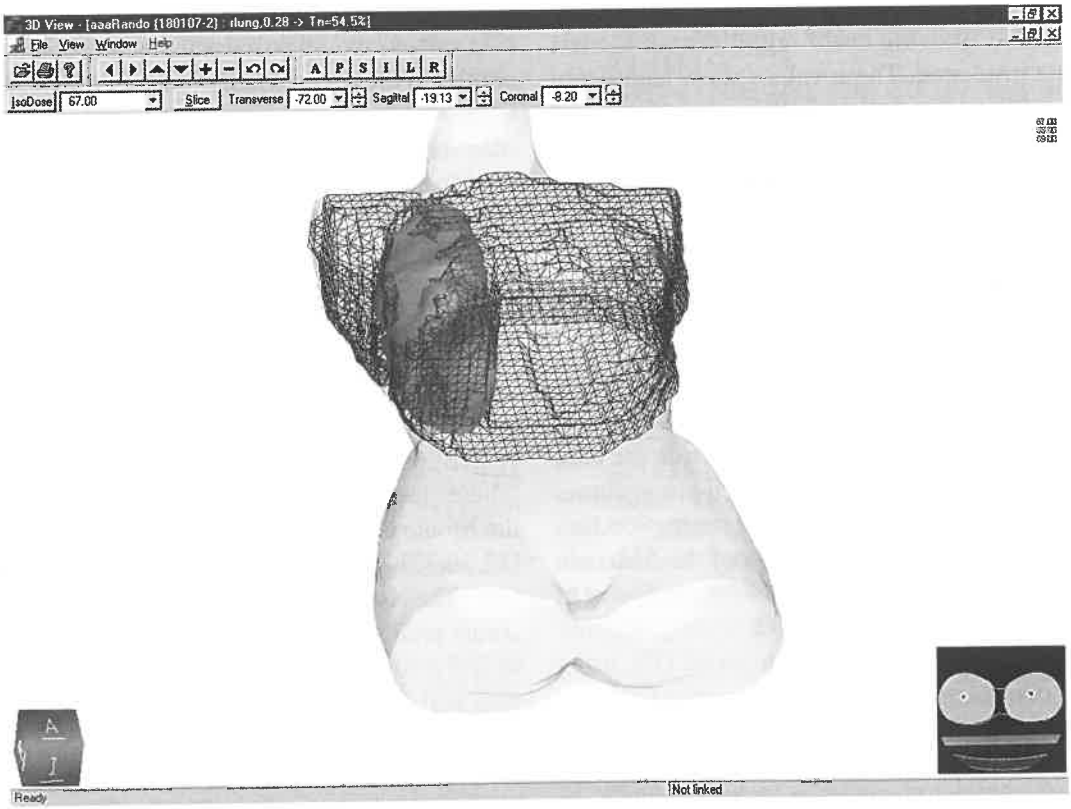


Figure 9. 3D view of 67% isodose surface in the right lung of the Alderson phantom. It was obtained with the use of a 10 mm lead, lung shaped attenuator (T_n= 52%). 3D views allow identifying regions of high and low doses inside the lung.

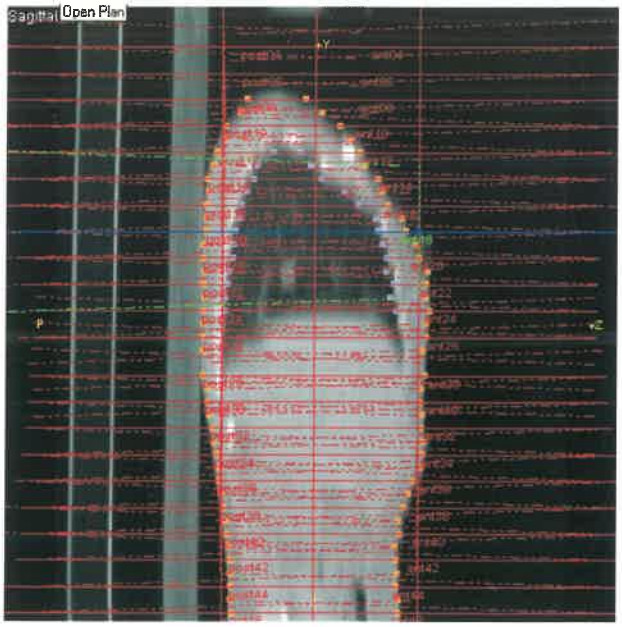


Figure 10. Typical example of the stationary beams used in the "moving beam" approach (sagittal view).

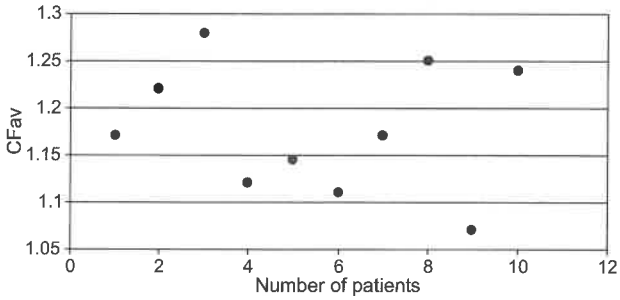


Figure 11. CF_{av} of the right lung for 10 of the patients studied. The variation in the CF_{av} values is obvious.

beams setting and TPS computations. The average lung correction factors (CF_{av}) obtained by the two methods differed by < 2%, showing that either approach can be applied.

Figure 11 shows the average right lung CFs obtained with the "moving beam" approach for the last 10 patients irradiated. These values show significant variation attributed to patients' external contours and lung anatomical differences. Therefore, a general, non patient-specific, lung CF_{av} is not applicable.

Discussion

The results presented show that the method implemented may be used to estimate the relative midline lung dose in TBI translation technique with an error of $\leq \pm 3\%$. Dose computations anywhere inside the lung except at the soft tissue/lung interface are accurate to within 5%. The midline lung dose correction factor (CF_o) for the central lung section of the Alderson phantom computed by the TPS is 1.14 for a field size of 40×40 cm at a lung depth of about 8 cm. Lung inhomogeneity corrections in TBI with commercial TPS, using the ETAR correction algorithm, have led to a lung correction factor of 1.17±3% [16,17]. This correction factor refers to a Co-60 unit for a field size of 50×60 cm at a lung depth of 9 cm. The value at a lung depth of 8 cm and a 40×40 cm field size, however, may be estimated from the above value using literature data [35] (Table 3) and is in the area of 1.14-1.15, a value that is in good agreement with our results.

Measurements under TBI conditions with a 4MV linear accelerator have led to overall lung CFs of 1.03-1.12 [12], reflecting the effect of the anatomy of the lung. In our case, the CF variation referring to the entire lung was 1.02-1.14.

The value of narrow beam lead attenuation coefficient affects the TPS calculations. Our value was smaller by about 2.5% compared with that obtained by Van Dyk by extrapolation to zero field size [32]. For a 10 mm lead filter, this results in T_n=51%, which is equally good for producing the desired lung isodose of 67%.

Broad beam attenuation coefficients (or transmission values) should be measured under conditions very similar to the actual irradiation geometry. Differences in measurement geometry, even for the same field size, may result in transmission errors of several percents. Attenuation data for a given field size should not be used for field sizes that differ significantly. For instance, if attenuation data for a 40×40 cm field are used for a 50×50 cm field, the error in the transmission value for 10-12 mm of lead will be around 3% [18].

If CT scan data are used and the ETAR algorithm is applied for inhomogeneity corrections, then the dose distribution may be obtained with an accuracy of 3% [16,18]. For better accuracy including the lung areas where electronic equilibrium is not established, either the Monte Carlo or convolution methods are required [12,36,37].

The computed average lung dose is used as an accurate estimate of the required beam filtration. However, due to lung anatomy, an attenuator of constant thickness will overprotect and underprotect certain parts of the lung for the same average lung dose. Thickness modifications would take lung thickness variation into account resulting in varying thickness attenuators. The latter has been applied to many patients.

In our approach the variation in patient thickness

in the AP direction is drastically reduced with bolus material. This difficulty has been acknowledged and a variable speed translating couch that takes the body contour differences into account has been employed instead [38].

In our method appropriately shaped electron beams of suitable energy are used to compensate for the reduced dose to thoracic wall due to lung attenuators. Use of the TPS enables the study of the combined effect of dose distributions from photons and electrons.

A drawback of the method is the fact that the attenuator shadow, obtained using a stationary geometry and the BEV facility, is different from that obtained in the actual patient translation technique. For the moving beam, the geometric penumbra at the edges of the attenuator is increased by one order of magnitude (from the order of the mm to a few cm) with a dose increase that extends under the attenuator edges. This effect has been verified experimentally for a 6 MV linear accelerator. An increase in the penumbra near the filter edge from < 0.5 cm (stationary beam) to > 3 cm (moving beam) has been measured [39].

Studies in mice have shown that the apex of the lung seems to be less sensitive to radiation than the base [40]. This is not the case, however, at the other end of the attenuator that covers the base of the lung. Using a lung attenuator that moves at an appropriate speed in opposite direction to that of the couch can solve this problem [41]. Alternatively, reducing the length of the irradiation field will proportionally decrease the penumbra at the expense of irradiation time and patient's convenience. For this reason, the field length is currently set to 30 cm. Also, use of a half-beam block in the craniocaudal direction combined with suitable couch direction of movement can eliminate the penumbra effect.

References

1. Lawton CA, Barber-Derus S, Murray KJ et al. Technical modifications in hyperfractionated total body irradiation for T-lymphocyte depleted bone marrow transplant. Int J Radiat Oncol Biol Phys 1989; 17: 319-322.
2. Weshler Z, Breuer R, Or R et al. Interstitial pneumonitis after total body irradiation; effect of partial lung shielding. Br J Haematol 1990; 74: 61-64.
3. Down JD, Tarbell NJ, Thames HD, Mauch PM. Syngeneic and allogeneic bone marrow engraftment after total body irradiation dependence on dose, dose rate and fractionation. Blood 1991; 77: 661-669.
4. Latini P, Aristei C, Aversa F et al. Lung damage following bone marrow transplantation after hyperfractionated total body irradiation. Radiother Oncol 1991; 22: 127-132.
5. Molls M, Bamberg M, Beelen DW, Mahmoud HK, Quast U, Schaefer UW. Different TBI procedures in Essen: Results and clinical considerations on the risk of leukaemic relapse and interstitial pneumonitis. Strahlenther Onkol 1987; 163: 237-240.
6. Molls M, Quast U, Schaefer UW et al. Clinical results and the Essen concept of TBI. Radiother Oncol 1990; 18 (Suppl 1): 121-124.
7. Quast U. Physical treatment planning for total body irradiation- Patient translation and beam zone method. Med Phys 1985; 12: 567-573.
8. Miralbell R, Rouzaud M, Grob E et al. Can a total body irradiation technique be fast and reproducible? Int J Radiat Oncol Biol Phys 1994; 29: 1167-1173.
9. Briot E, Dutrex A, Bridier A. Dosimetry for total body irradiation. Radiother Oncol 1990; 18 (Suppl 1): 16-29.
10. Fluhs D, Quast U, Szy D. Systematic measurements of lung dose. Strahlenther Onkol 1991; 167: 147-148.
11. Marinello G, Barrie AM, Le Bourgeois JP. Measurement and calculation of lung dose in total body irradiation performed with a Co-60 unit. J Eur Radiother 1982; 3: 174-182.
12. Mijnheer BJ, Rice RK, Chin LM. Lung dose measurements performed at the joint center for radiation therapy, Boston, USA. Strahlenther Onkol 1991; 167: 135-151.
13. Planskoy B, Tapper P D, Bedford AM, Davis FM. Physical aspects of total body irradiation at the Middlessex Hospital (UCL group of hospitals), London 1988-1993: II: In vivo planning and dosimetry. Phys Med Biol 1996; 41: 2327-2343.
14. Quast U. Dosimetry of total body irradiation: a review. "Dosimetry in Radiotherapy". Proceedings of an International Symposium on Dosimetry in Radiotherapy organised by the International Atomic Energy Agency in co-operation with the World Health Organisation. Vienna, 31 August- 4 September 1987, Vol 2, pp 187-210.
15. Quast U. The dose to lung in TBI. Strahlenther Onkol 1991; 167: 135-151.
16. Van Dyk J, Battista JJ, Rider WD. Half body radiotherapy: The use of computed tomography to determine dose to lung. Int J Radiat Oncol Biol Phys 1980; 6: 463-470.
17. Van Dyk J. Dosimetry for total body irradiation. Radiother Oncol 1987; 9: 107-118.
18. Van Dyk J, Galvin JM, Glasgow GP, Podgorsak EB. The physical aspects of total and half body photon irradiation. AAPM, TG 29, Radiation Therapy committee AAPM report No17, 1986.
19. Van Dyk, J. Lung dose calculations using computerised tomography: Is there a need for pixel based procedures? Int J Radiat Oncol Biol Phys 1983; 9: 1035-1041.
20. Van Dyk J. Magna field irradiation: Physical considerations. Int J Radiat Oncol Biol Phys 1983; 9: 1913-1918.
21. Christ G. In vivo dosimetry for TBI. Strahlenther Onkol 1987; 163: 220-221.
22. Christ G, Well JC, Nuslin F. In vivo dosimetry for TBI. Strahlenther Onkol 1991; 167: 135-151.
23. Duch MA, Ginjaume M, Chakkor H, Ortega X, Jornet N, Ribas M. Thermoluminescence dosimetry applied to in vivo dose measurements for total body irradiation techniques. Radiother Oncol 1998; 47: 319-324.
24. Hussein S, Kennelly GM. Lung compensation in total body irradiation: a radiographic method. Med Phys 1996; 23: 357-360.
25. Quast U. Summary of the discussion on in vivo dosimetry. J Eur Radiother 1982; 3: 250-261.
26. Scalchi P, Francenson P. Calibration of a mosfet detection

system for 6-MV in vivo dosimetry. Int J Radiat Oncol Biol Phys 1998; 40: 987-993.
27. Umek B, Zwitter M, Habic H. Total body irradiation with translation method. Radiother Oncol 1996; 38: 253-255.
28. Aget H, Van Dyk J, Leung PMK. Utilization of a high-energy photon beam for whole body irradiation. Radiology 1977; 123: 747-751.
29. Lam WC, Lindskong BA, Order SE, Grant DG. The dosimetry of Cobalt-60 for total body irradiation. Int J Radiat Oncol Biol Phys 1979; 5: 905-911.
30. THERAPLAN plus, version 2.1, System Administrator's Manual, Unit Modelling Algorithms.
31. Kalef-Ezra JA, Karantanas AH, Koligliatis T, Boziari A, Tsekeris P. Electron density of tissues and breast cancer radiotherapy: a quantitative CT study. Int J Radiat Oncol Biol Phys 1998; 41: 1209-1214.
32. Van Dyk J. Broad beam attenuation of cobalt-60 gamma rays and 6,18 and 25 x rays by lead. Med Phys 1986; 12: 105-110.
33. Quast U. Dosimetry and treatment planning of total body irradiation. Lecture on EFOMP Summer School in La Rapida, Spain, 1992.
34. Rice RK, Hansen JL, Chin LM, Mijnheer BJ, Bjarngard BE. The influence of ionisation and phantom design on the measurement of lung dose in photon beams. Med Phys 1988; 15: 884-890.
35. McDonald SC, Keller BE, Rubin P. Method for calculating dose when lung tissue lies in the treatment field. Med Phys 1976; 3: 210-216.
36. Ahnesjo A. Collapsed cone convolution. A 3D convolution method for photon dose calculation in heterogeneous media. Strahlenther Onkol 1991; 167: 144-145.
37. Reinhardt S. Dose calculation by Monte Carlo methods in inhomogeneous media. Strahlenther Onkol 1991; 167: 143-144.
38. Chretien M, Cote C, Blais R, Roy-Lacronix L, Larochelle M. A variable speed translating technique for total body irradiation. Med Phys 2000; 27: 1127-1130.
39. Sarfarez M, Yu C, Chen DJ, Der L. A translational couch technique for total body irradiation. J Appl Clin Med Phys 2001; 2: 201-209.
40. Liao ZX, Travis EL, Tucker SL. Damage and morbidity from pneumonitis after irradiation of partial volumes of mouse lung. Int J Radiat Oncol Biol Phys 1995; 32: 1359-1370.
41. Papiez L, Montebello J, DesRosiers C, Papiez E. The clinical application of dynamic shielding and imaging in moving table total body irradiation. Radiother Oncol 1999; 51: 219-224.